

Optomechanical effects of two-level systems in a back-action evading measurement of micro-mechanical motion

J. Suh, A. J. Weinstein, and K. C. Schwab

Citation: *Appl. Phys. Lett.* **103**, 052604 (2013); doi: 10.1063/1.4816428

View online: <http://dx.doi.org/10.1063/1.4816428>

View Table of Contents: <http://apl.aip.org/resource/1/APPLAB/v103/i5>

Published by the [AIP Publishing LLC](#).

Additional information on *Appl. Phys. Lett.*

Journal Homepage: <http://apl.aip.org/>

Journal Information: http://apl.aip.org/about/about_the_journal

Top downloads: http://apl.aip.org/features/most_downloaded

Information for Authors: <http://apl.aip.org/authors>

ADVERTISEMENT



Optomechanical effects of two-level systems in a back-action evading measurement of micro-mechanical motion

J. Suh, A. J. Weinstein, and K. C. Schwab^{a)}

Applied Physics, California Institute of Technology, Pasadena, California 91125, USA

(Received 29 April 2013; accepted 3 July 2013; published online 29 July 2013)

We show that the two-level systems (TLS) in lithographic superconducting circuits act as a power-dependent dielectric leading to non-linear responses in a parametrically coupled electromechanical system. Driven TLS shift the microwave resonance frequency and modulate the mechanical resonance through the optical spring effect. By pumping with two tones in a back-action evading measurement, these effects produce a mechanical parametric instability which limits single quadrature imprecision to $1.4 x_{zp}$. The microwave resonator noise is also consistent to a TLS-noise model. These observations suggest design strategies for minimizing TLS effects to improve ground-state cooling and quantum non-demolition measurements of motion. © 2013 AIP Publishing LLC. [<http://dx.doi.org/10.1063/1.4816428>]

Parametrically coupled electromechanical systems have been explored for over 30 years^{1,2} in a wide range of mass and length scales. They have been utilized as ultra-sensitive force transducers for the detection of gravitational waves and more recently for the exploration of quantum limits and quantum states of motion.³ Furthermore, continuous measurements of position have reached the regime of back-action limited resolution,^{4,5} motivating the implementation of back-action evading (BAE) techniques.^{6,7}

It is typically assumed that only mechanical and electromagnetic resonator coordinates are relevant in the dynamics of the electromechanical systems. However, it is also well understood that solid-state devices have many other degrees of freedom that significantly affect the system such as two-level systems (TLS) in amorphous oxides. This is especially important for micron-scale systems where oxide coatings on surfaces can contribute a substantial fraction of the transducer volume. TLS were first proposed as a model to explain anomalous specific heat and thermal conductivity of amorphous silicon oxides at low temperatures.^{8,9} Subsequent acoustic and microwave measurements also have verified the model.^{10,11} It is generally accepted that O-H bonds in the oxide are one of the microscopic origins for such TLS.¹²

The TLS in amorphous oxides are found to be ubiquitous in solid-state quantum devices such as superconducting qubits,¹³ optical,¹⁴ and microwave resonators,¹⁵ leading to qubit decoherence and excess phase noise. In addition, coupling a mechanical resonator to a single engineered TLS in the dispersive-limit^{16,17} and the resonant limit¹⁸ has been explored; what we show here complements this work and is in the limit of a large number of natural TLS showing both resonant absorption and off-resonant dispersive effects.

Our electromechanical system is composed of a radio-frequency micromechanical resonator tightly coupled to a lithographic superconducting microwave resonator, which realizes a mechanical harmonic oscillator whose position modulates the frequency of a high frequency electromagnetic

resonator. In addition to showing strong electromechanical coupling, formally identical to the optomechanical interaction via radiation pressure,¹⁹ this device provides a unique opportunity to simultaneously study acoustic and electromagnetic TLS effects compared to previously studied microwave devices.¹⁵

As shown in Fig. 3, we find that the microwave resonance frequency has a power-dependent shift that pulls the mechanical resonance via a strong optical spring effect. In a two-tone BAE measurement for a single mechanical quadrature measurement,⁶ the beating of microwave power results in the modulation of the effective spring constant at twice the mechanical resonance frequency. In the strong measurement limit approaching zero-point motion sensitivity, this modulation can produce a parametric instability for the mechanical motion.

In this work, the mechanical resonator is a silicon nitride membrane ($40 \mu\text{m} \times 40 \mu\text{m} \times 100 \text{nm}$), coated by a 60 nm thick layer of aluminum (Al), with a fundamental resonance at 3.7 MHz ($=\omega_m/2\pi$) and a damping rate of 50 s^{-1} ($=\gamma_{m0}/2\pi$) below 100 mK. We estimate its zero-point motion $x_{zp} = \sqrt{\hbar/2m\omega_m} \approx 1.7 \text{ fm}$, where \hbar is the reduced Planck constant and m is the effective mass of the mechanical resonator. A capacitor is formed by a top gate separated by approximately 100 nm (Fig. 1(a)). This electromechanical capacitor is connected in parallel with a spiral inductor to form a superconducting LC resonator with resonance frequency of 5.3 GHz ($=\omega_{LC}/2\pi$), internal damping rate of $2.6 \times 10^5 \text{ s}^{-1}$ ($=\kappa/2\pi$), input and output damping rate of $8 \times 10^4 \text{ s}^{-1}$ ($=\kappa_{in}/2\pi, \kappa_{out}/2\pi$), and circuit impedance $Z_0 = \sqrt{L/C} \approx 200 \Omega$. The membrane motion modulates the capacitor with a parametric coupling of $g = \partial\omega_{LC}/\partial x = 2\pi \times 5.1 \text{ MHz/nm}$. The measurement schematic is presented in Fig. 1(b), similar to Ref. 6. Shot-noise limited microwave sources pump the circuit, implemented with filtering at room temperature and attenuation at cryogenic temperatures. After the LC resonator, the signal passes through cryo-circulators and is amplified by a cryo-amplifier at 4 K before being analyzed with a spectrum analyzer. To calibrate coupling and losses, a single tone is

^{a)}schwab@caltech.edu

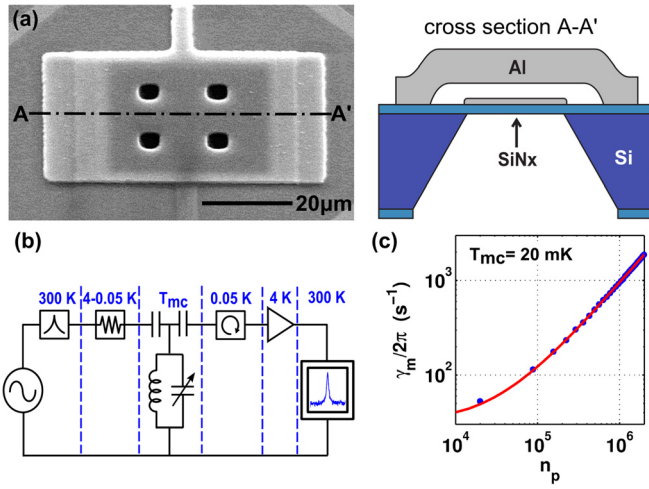


FIG. 1. Device and optomechanical coupling. (a) (Left) Sample electron micrograph showing the electromechanical capacitor formed by silicon nitride (SiNx) membrane and Al top gate. An Al spiral inductor (not shown) completes the microwave LC resonator. (Right) Sideview of structure. (b) Measurement schematic. (c) Mechanical damping rate vs. number of pump photons. The solid line is a fit to optical damping.

placed at $\omega_p = \omega_{LC} - \omega_m$, which increases the mechanical damping rate due to photon back-action, so called optical damping.¹⁹ Figure 1(c) is the result of such measurement where n_p is the number of pump photons in the LC resonator with a fit to optical damping.

A series of measurements on the microwave and mechanical resonator shows evidence of two-level systems (Fig. 2). According to TLS model,^{20–22} the dielectric constant of an amorphous solid with TLS at ω_{LC} behaves as

$$\epsilon_{TLS}(\omega_{LC}) = \frac{Pd_0^2}{3} \int_0^{\omega_{max}} d\omega \tanh\left(\frac{\hbar\omega}{2k_B T}\right) \times \frac{1 + (\omega - \omega_{LC})^2 T_2^2}{1 + \Omega^2 T_1 T_2 + (\omega - \omega_{LC})^2 T_2^2} \times \left(\frac{1}{\omega - \omega_{LC} + j/T_2} + \frac{1}{\omega + \omega_{LC} - j/T_2} \right), \quad (1)$$

where k_B is the Boltzmann constant and T is the temperature, with TLS parameters as P : density of states, d_0 : average dipole moment, Ω : average TLS Rabi frequency ($= \frac{2d_0}{\sqrt{3\hbar}}|E|$ for electric field strength $|E|$), T_1 : relaxation time, T_2 : dephasing time, and ω_{max} : cut-off transition frequency. For an amorphous solid with TLS occupying volume V_h with a dielectric constant ϵ_h , a filling factor F is defined as the ratio of the microwave energy in V_h over that in the whole system. We approximate the real part of Eq. (1) for microwave resonance shift $\Delta\omega_{LC}$ in a weak driving regime ($\Omega^2 T_1 T_2 \ll 1$) resulting in

$$\frac{\Delta\omega_{LC}}{\omega_{LC}} \simeq \frac{F\delta_{TLS}}{\pi} \left(\text{Re}\Psi\left(\frac{1}{2} - \frac{\hbar\omega_{LC}}{2\pi j k_B T}\right) - \log\frac{\hbar\omega_{max}}{2\pi k_B T} \right), \quad (2)$$

where Ψ is the digamma function and $\delta_{TLS} = \pi P d_0^2 / 3\epsilon_h$. The imaginary part of Eq. (1) gives rise to microwave dissipation $\delta_{LC} = \kappa / \omega_{LC}$

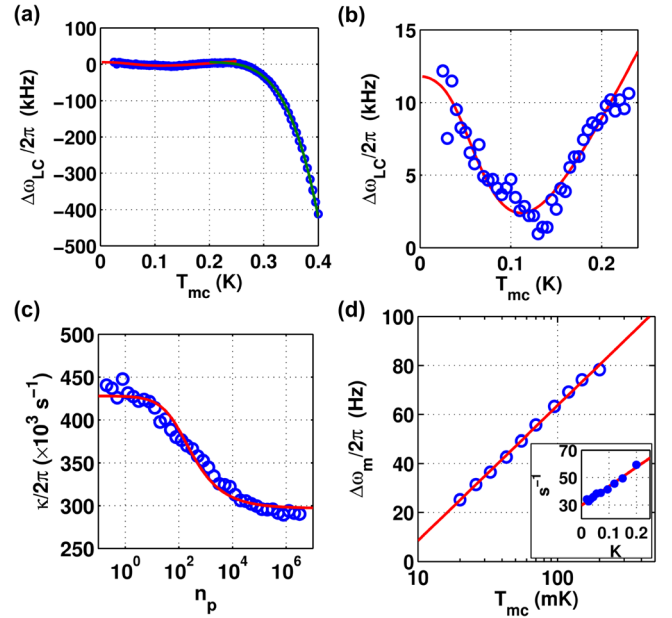


FIG. 2. Evidence of TLS. (a) and (b) Microwave resonance shift vs. temperature. (a) Above 0.2 K, the data fit to BCS theory⁴⁰ (green line). (b) At lower temperatures, a fit to TLS model (Eq. (2)) matches to the observed shift (red line). (c) Microwave damping rate vs. number of pump photons. The red line is a fit to the TLS model (Eq. (3)) with a constant offset ($3 \times 10^5 \text{ s}^{-1}$) from non-TLS contributions. (d) Mechanical resonance shift vs. temperature with a TLS model fit to Eq. (4). (Inset) Mechanical damping rate shows a linear behavior over temperature.

$$\delta_{LC} \simeq \frac{F\delta_{TLS} \tanh(\hbar\omega_{LC}/2k_B T)}{\sqrt{1 + \Omega^2 T_1 T_2}}. \quad (3)$$

Our microwave resonance data fit well with the predictions of Eqs. (2) and (3) as shown in Figs. 2(b) and 2(c). Both of these independent measurements result in $F\delta_{TLS} \approx 2.5 \times 10^{-5}$. In our design, the electric field is well-confined inside the electromechanical capacitor, hence we approximate the filling factor as the TLS contribution from amorphous aluminum oxide (AlOx) on Al inside the capacitor gap. Ref. 13 identifies the TLS loss tangent as $\delta_{TLS} \approx 1.6 \times 10^{-3}$ for AlOx. Using this value for the loss tangent, $F \approx 1.6 \times 10^{-2}$. This corresponds to a $\sim 8 \text{ nm}$ oxide layer coating each Al plate ($\epsilon_h \approx 10$) which is consistent with typical thicknesses of native oxide ($\sim 4 \text{ nm}$).²³ As measured in Fig. 2(b), the behavior of the damping rate at high occupation provides additional information from the saturation factor $\sqrt{1 + \Omega^2 T_1 T_2}$. Because the TLS Rabi frequency $\Omega \propto \sqrt{n_p}$, we can define a critical number of pump photons n_{crit} for saturation as $n_p/n_{crit} = \Omega^2 T_1 T_2$. The fit results $n_{crit} = 96$. This corresponds to a critical electric field $E_c \approx 69 \text{ V/m}$ which is consistent with data from superconducting coplanar waveguide resonators.²⁴

In addition, TLS interacting with phonons changes the speed of sound v over temperature T as^{20,25}

$$\frac{\Delta v}{v} = \frac{PM^2}{\rho v^2} \log\left(\frac{T}{T_0}\right), \quad (4)$$

in a low frequency limit ($\hbar\omega \ll k_B T$), where v is the speed of sound, M is the deformation potential, and T_0 is a reference

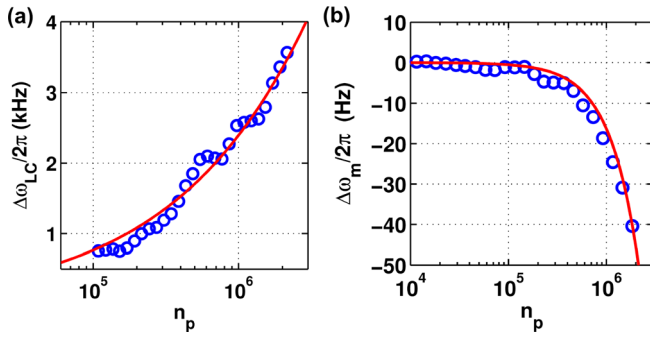


FIG. 3. TLS-induced microwave shift and optical spring. (a) Microwave resonance frequency shifts over n_p . The solid line is a fit to the TLS model in strong driving regime, Eq. (1). (b) Mechanical resonance frequency also shifts, agreeing well with a prediction of optical spring calculated from solid line in (a).

temperature. In Fig. 2(d), we plot the thermal shift of the mechanical resonance frequency, which is proportional to the speed of sound. The data fit well to the logarithmic behavior of Eq. (4). Since SiNx is the dominant contributor to the membrane tension and determines mechanical resonance frequency, we expect P to reflect the TLS density in SiNx. With $M = 0.32$ eV,²⁵ $\rho = 3200$ kg/m³, and $v = 9200$ m/s, we estimate $P \sim 7 \times 10^{44}$ J⁻¹ m⁻³. This TLS density measured in an acoustic measurement can also predict TLS-limited SiNx microwave loss.²¹ Since SiNx does not involve oxygen during deposition, its TLS are expected to have little O-H bond contribution. In a photon echo measurement,¹¹ intrinsic TLS excluding O-H is found to have dipole moment of 2×10^{-30} C-m. Adopting this value as the dipole moment for the TLS of SiNx, we estimate $\delta_{TLS} \approx 4 \times 10^{-5}$ for SiNx. This is consistent with Ref. 13, where the loss tangent of SiNx was $\sim 5 \times 10^{-5}$, about 30 times lower than silicon oxide. In mechanical damping rates, however, we note a deviation from TLS theory (Fig. 2(d) inset). Since the normal electron density is highly suppressed in superconducting aluminum, we expect the TLS relaxation rate is dominated by phonon processes, and therefore, $\gamma_{m0} \propto T^3$. In contrast, the observed dependence is close to $\gamma_{m0} \propto T$, similar to what has been observed in single crystal silicon resonators.²⁶ This deviation might indicate that either the mechanical damping rate is dominated by other temperature-dependent sources or the TLS relaxation rate is modified by the phonon density of states in a quasi-2D system such as the thin membrane studied here.

In a strong driving regime ($\Omega^2 T_1 T_2 > 1$), TLS have a power-dependent dielectric constant, as seen in Eq. (1), which can be viewed as a Kerr-like nonlinearity.²⁷ In our experiment, this is observed by the frequency shift of microwave resonance at high n_p as shown in Fig. 3(a). Using the previously discussed AlOx TLS parameters, a fit to a numerical integration of Eq. (1) results in the solid line.²⁸ From the fit, we get $T_2 \approx 63$ ns, close to typical values observed in phase qubits.²⁹ This power-dependent shift of the microwave resonance affects the mechanical resonance via optomechanical coupling. In Fig. 3(b), we plot the measured mechanical resonance shift and an estimate derived from the fitted microwave resonance shift in (a) and the optical spring effect^{19,28}

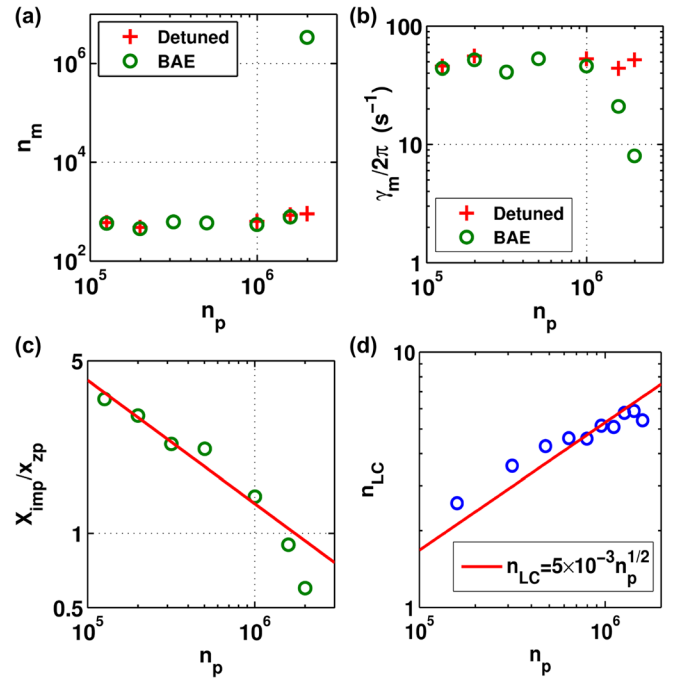


FIG. 4. (a)–(c) Two-tone BAE measurements and parametric instability. Red crosses are from detuned two-tone measurements,^{6,7} and green circles are from BAE measurements. (a) The average occupation number of the mechanical resonator in the BAE measurement shows abrupt increase above $n_p \approx 2 \times 10^6$, whereas such instability is absent in the detuned two-tone measurements. (b) In BAE, the mechanical damping rates also drop significantly accompanying the increase in n_m . In the detuned two-tone measurements, there is no sign of such linewidth narrowing. (c) The quadrature imprecision in BAE reaches $1.4x_{zp}$ before parametric instability. (d) The average occupation number of LC resonator (n_{LC}) vs. number of pump photons. The pumped LC resonator becomes populated with noise power, which is quantified by the average occupation number n_{LC} . It shows reasonable agreement to $n_p^{1/2}$ dependence.

$$\Delta\omega_m = \sum_{n=r,b} \frac{2g^2 x_{zp}^2 n_p \Delta_n (\Delta_n^2 - \omega_m^2 + (\kappa/2)^2)}{(\Delta_n^2 - \omega_m^2)^2 + 2(\kappa/2)^2 (\Delta_n^2 + \omega_m^2) + (\kappa/2)^4}, \quad (5)$$

where $\Delta_{r,b} = \omega_{r,b} - \omega_{LC}$. From Eq. (5), we expect $\Delta\omega_m \simeq 0$ with two tones symmetrically placed ($\Delta_b = -\Delta_r = \omega_m$) in an ideal two-tone BAE.³⁰ However, TLS induced power-dependent frequency shift leads to pump detuning and non-zero optical spring. Furthermore, two-tone BAE imposes harmonic time-dependence in n_p as $n_p = n_{p0}(1 + \cos(2\omega_m t))$ and $\Delta\omega_m$ becomes modulated by $2\omega_m$.

The modulation of ω_m at $2\omega_m$ satisfies the condition of degenerate parametric amplification and oscillation.³¹ This parametric instability has been the major challenge in achieving BAE below zero-point uncertainty.^{6,7} In our BAE measurements shown in Fig. 4, we observe an instability at n_p above $\sim 2 \times 10^6$, as evidenced by sudden increase in the average number of mechanical occupation n_m and a sharp drop in γ_m accompanied to that. These observations are consistent to the frequency shift measurements in Fig. 3. The amplified quadrature in the parametric amplification has gain of $G = 1/(1 - \Delta\omega_m/\gamma_{m0})$, where γ_{m0} is the initial line width of mechanical resonator with no parametric drive.³¹ From Fig. 3(b), we expect $G \rightarrow \infty$ at $n_p \approx 2 \times 10^6$, which matches well with data in Fig. 4. This defines the ultimate limit in the quadrature imprecision in our BAE measurements at $1.4x_{zp}$.

In addition to the microwave nonlinearity, TLS have been suggested as a source of excess phase noise in superconducting coplanar resonators.³² In our detuned pump configuration, the frequency noise of the LC resonator generates noise power in the sidebands of the pumps, exciting the LC resonator. We quantify the total noise power inside the resonance by an average occupation number n_{LC} , which is defined by $n_{LC} = P_{LC}/(\hbar\omega_{LC}\kappa_{out})$ with P_{LC} as the total noise power under the LC resonance at the output port. By extrapolating $1/f^{1/2}$ part of the phase noise curve in Ref. 32 to estimate the noise at the detuning of ω_m ,²⁸ we arrive at $n_{LC} \approx 4 \times 10^{-2} n_p^{1/2}$. This $n_p^{1/2}$ power law agrees to our observations reasonably well and its coefficient is also within an order of magnitude as shown in Fig. 4(d), which suggests that the TLS noise model³² might be also valid in our electromechanical system. In on-going efforts of exploring quantum electromechanical resonators with superconducting microwave resonators,^{33–35} the microwave noise at high pump power has been limiting the lowest possible thermal occupation of mechanical modes. Our result indicates TLS might be one of the sources of such noise. It might be possible to reduce this noise contribution by engineering the TLS density with nitride superconductors,³⁶ modifying resonator structure to minimize TLS filling factor,³⁷ or utilizing magnetic coupling to mechanical motion³⁸ which is less sensitive to electric dipole moments of TLS.

In summary, for a micro-electromechanical system parametrically coupled to a superconducting LC resonator, we observe a TLS-induced power-dependent shift in the microwave resonance frequency and an associated mechanical resonance frequency shift from the optomechanical coupling. The TLS parameters are consistent with values from the previous reports,^{13,15,29} fitting the observations well within the TLS model generally accepted for solid-state superconducting devices. In two-tone BAE measurements, the mechanical resonance shift becomes modulated at twice the resonance leading to a parametric instability near zero-point imprecision. The microwave noise power is also observed to match with a TLS-based model³² prediction. In light of the previous research on TLS in qubits and superconducting resonators, we expect that improvements in both material and design will lead to the goal of true quantum non-demolition measurements of mechanical motion.³⁹

We acknowledge funding provided by the Institute for Quantum Information and Matter, an NSF Physics Frontiers Center with support of the Gordon and Betty Moore Foundation (NSF-IQIM 1125565), by DARPA (DARPA-QUANTUM HR0011-10-1-0066), and by NSF (NSF-DMR 1052647 and NSF-EEC 0832819).

¹V. B. Braginsky and F. Y. Khalili, *Quantum Measurement* (Cambridge, 1995).

²M. F. Bocko and R. Onofrio, *Rev. Mod. Phys.* **68**, 755 (1996).

³M. Aspelmeyer, P. Meystre, and K. Schwab, *Phys. Today* **65**(7), 29 (2012).

- ⁴A. Naik, O. Buu, M. D. LaHaye, A. D. Armour, A. A. Clerk, M. P. Blencowe, and K. C. Schwab, *Nature (London)* **443**, 193 (2006).
- ⁵T. P. Purdy, R. W. Peterson, and C. A. Regal, *Science* **339**, 801 (2013).
- ⁶J. B. Hertzberg, T. Rocheleau, T. Ndukum, M. Savva, A. A. Clerk, and K. C. Schwab, *Nat. Phys.* **6**, 213 (2010).
- ⁷J. Suh, M. D. Shaw, H. G. LeDuc, A. J. Weinstein, and K. C. Schwab, *Nano Lett.* **12**, 6260 (2012).
- ⁸P. W. Anderson, B. I. Halperin, and C. M. Varma, *Phil. Mag.* **25**, 1 (1972).
- ⁹W. A. Phillips, *J. Low Temp. Phys.* **7**, 351 (1972).
- ¹⁰B. Golding and J. E. Graebner, *Phys. Rev. Lett.* **37**, 852 (1976).
- ¹¹B. Golding, M. v. Schickfus, S. Hunklinger, and K. Dransfeld, *Phys. Rev. Lett.* **43**, 1817 (1979).
- ¹²M. v. Schickfus and S. Hunklinger, *J. Phys. C* **9**, L439 (1976).
- ¹³J. M. Martinis, K. B. Cooper, R. McDermott, M. Steffen, M. Ansmann, K. D. Osborn, K. Cicak, S. Oh, D. P. Pappas, R. W. Simmonds *et al.*, *Phys. Rev. Lett.* **95**, 210503 (2005).
- ¹⁴R. Rivière, S. Deléglise, S. Weis, E. Gavartin, O. Arcizet, A. Schliesser, and T. J. Kippenberg, *Phys. Rev. A* **83**, 063835 (2011).
- ¹⁵J. Gao, M. Daal, A. Vayonakis, S. Kumar, J. Zmuidzinas, B. Sadoulet, B. A. Mazin, P. K. Day, and H. G. Leduc, *Appl. Phys. Lett.* **92**, 152505 (2008).
- ¹⁶M. D. LaHaye, J. Suh, P. M. Echternach, K. C. Schwab, and M. L. Roukes, *Nature (London)* **459**, 960 (2009).
- ¹⁷J. Suh, M. D. LaHaye, P. M. Echternach, K. C. Schwab, and M. L. Roukes, *Nano Lett.* **10**, 3990 (2010).
- ¹⁸A. D. O'Connell, M. Hofheinz, M. Ansmann, R. C. Bialczak, M. Lenander, E. Lucero, M. Neeley, D. Sank, H. Wang, M. Weides *et al.*, *Nature (London)* **464**, 697 (2010).
- ¹⁹F. Marquardt, J. P. Chen, A. A. Clerk, and S. M. Girvin, *Phys. Rev. Lett.* **99**, 093902 (2007).
- ²⁰S. Hunklinger and W. Arnold, *Physical Acoustics* (Academic, New York, 1976), Vol. 12.
- ²¹W. A. Phillips, *Amorphous Solids: Low-Temperature Properties* (Springer-Verlag, Berlin, New York, 1981).
- ²²J. Gao, "The physics of superconducting microwave resonators," Ph.D. thesis (California Institute of Technology, 2008).
- ²³R. K. Hart, *Proc. R. Soc. London, Ser. A* **236**, 68 (1956).
- ²⁴D. P. Pappas, M. R. Vissers, D. S. Wisbey, J. S. Kline, and J. Gao, *IEEE Trans. Appl. Supercond.* **21**, 871 (2011).
- ²⁵L. Piché, R. Maynard, S. Hunklinger, and J. Jäckle, *Phys. Rev. Lett.* **32**, 1426 (1974).
- ²⁶R. N. Kleiman, G. Agnolet, and D. J. Bishop, *Phys. Rev. Lett.* **59**, 2079 (1987).
- ²⁷B. Yurke and E. Buks, *J. Lightwave Technol.* **24**, 5054 (2006).
- ²⁸See supplementary material at <http://dx.doi.org/10.1063/1.4816428> for the details of data fitting method, optical spring effect, and TLS noise estimate.
- ²⁹Y. Shalibo, Y. Rofe, D. Shwa, F. Zeides, M. Neeley, J. M. Martinis, and N. Katz, *Phys. Rev. Lett.* **105**, 177001 (2010).
- ³⁰A. A. Clerk, F. Marquardt, and K. Jacobs, *New J. Phys.* **10**, 095010 (2008).
- ³¹D. Rugar and P. Grütter, *Phys. Rev. Lett.* **67**, 699 (1991).
- ³²J. Gao, M. Daal, J. M. Martinis, A. Vayonakis, J. Zmuidzinas, B. Sadoulet, B. A. Mazin, P. K. Day, and H. G. Leduc, *Appl. Phys. Lett.* **92**, 212504 (2008).
- ³³T. Rocheleau, T. Ndukum, C. Macklin, J. B. Hertzberg, A. A. Clerk, and K. C. Schwab, *Nature (London)* **463**, 72 (2010).
- ³⁴J. D. Teufel, T. Donner, D. Li, J. W. Harlow, M. S. Allman, K. Cicak, A. J. Sirois, J. D. Whittaker, K. W. Lehnert, and R. W. Simmonds, *Nature (London)* **475**, 359 (2011).
- ³⁵F. Massel, S. U. Cho, J.-M. Pirkkalainen, P. J. Hakonen, T. T. Heikkilä, and M. A. Sillanpää, *Nat. Commun.* **3**, 987 (2012).
- ³⁶H. G. Leduc, B. Bumble, P. K. Day, B. H. Eom, J. Gao, S. Golwala, B. A. Mazin, S. McHugh, A. Merrill, D. C. Moore, O. Noroozian, A. D. Turner, and J. Zmuidzinas, *Appl. Phys. Lett.* **97**, 102509 (2010).
- ³⁷O. Noroozian, J. Gao, J. Zmuidzinas, H. G. LeDuc, and B. A. Mazin, *AIP Conf. Proc.* **1185**, 148 (2009).
- ³⁸H. J. Paik, *J. Appl. Phys.* **47**, 1168 (1976).
- ³⁹C. M. Caves, K. S. Thorne, R. W. P. Drever, V. D. Sandberg, and M. Zimmermann, *Rev. Mod. Phys.* **52**, 341 (1980).
- ⁴⁰D. C. Mattis and J. Bardeen, *Phys. Rev.* **111**, 412 (1958).